



Occurrence, mineral chemistry and origin of dumortierite in Ali Javad porphyry Cu-Au deposit, Sheivar Dagh alteration system, NW Iran

Fazel Khaleghi ^{*,1} and Zahra Karimzadeh ²

¹Department of Geology Tabriz Branch, Islamic Azad University, Tabriz, IRAN

²Department of Geology, Islamic Azad University, Ahar Branch, Ahar, IRAN

ARTICLE INFO

Submitted: December 2018

Accepted: April 2019

Available on line: April 2019

* Corresponding author:

fazel_khaleghi@iaut.ac.ir

DOI: 10.2451/2019PM869

How to cite this article:

Khaleghi F. and Karimzadeh Z. (2019)
Period. Mineral. 88, 131-145

ABSTRACT

Dumortierite appears as massive aggregates with distinct blue colour in the advanced argillic and silicified zones of the Ali Javad porphyry Cu-Au deposit in the Sheivar Dagh area, NW Iran. Based on field and petrographic observations, this mineral is formed at the latest stages of the hydrothermal activities as a late mineralization phase. Dumortierite is studied here to constrain its potential for characterizing mineralization and prospecting of the Cu-Au porphyry deposit. Chemistry of dumortierite is studied for the first time in a Cu-Au porphyry system and is compared with other examples from the world. This mineral is formed within the subvolcanic dacite to quartz monzonite rocks of the Ali Javad area. A multidisciplinary approach including petrography as well as XRD, ICP-MS, FTIR and EMP analyses was used to characterize the dumortierite samples. The results of this study show that formation of Mg-poor dumortierite is strictly related to the magmatic-hydrothermal system of the Ali Javad porphyry deposit. As Sheivar pluton was crystallizing, light elements including boron were accumulated in the aqueous hydrothermal fluids, which invaded the overlying volcanic rocks and produced vast alteration zones and dumortierite crystallization.

Keywords: Dumortierite; Argillic Alteration; Ali Javad porphyry; Mineral chemistry; FTIR.

INTRODUCTION

Dumortierite is an aluminium oxyborosilicate (named after the French paleontologist, Eugene Dumortier), which appears in different rock types including pegmatites, aplites, felsic dykes and granitoids (Huijsmans et al., 1982). This mineral can be found as a product of late stage pneumatolitic or hydrothermal processes (Kerr and Jenney, 1935; Sabzehei, 1971; Black, 1973; Foit et al., 1989), as well as in regional metamorphic rocks (Schreyer et al., 1975; Vrána, 1979; Takahata and Uchiyama, 1985; Beukes et al., 1987; Chopin et al., 1995).

The dumortierite group comprises dumortierite ($\text{Al}_6\text{BSi}_3\text{O}_{16}(\text{O},\text{OH})_2$) and magnesiudumortierite ($\text{Mg}_6\text{BSi}_3\text{O}_{16}(\text{O},\text{OH})_2$), where \square denotes cation vacancy

(Pieczka et al., 2013). The crystal structure of dumortierite was first described by Golovastikov (1965) and further refined by Moore and Araki (1978) as a semi-regular planar structure. Four principle regions can be considered in the dumortierite structure: (1) $[\text{AlO}_3]$ chains of face-sharing octahedra (the Al1 sites) surrounded by “pinwheels” of six SiO_4 tetrahedra, two Si1 and four Si2 sites; (2) $[\text{Al}_4\text{O}_{12}]$ cubic close-packed chains, containing the Al2 and Al3 octahedral sites, that are joined to equivalent chains by reflection at the O1 corners of the Al2 octahedra to form $[\text{Al}_4\text{O}_{11}]$ sheets oriented parallel to (010); (3) $[\text{Al}_4\text{O}_{12}]$ double-chains containing the Al4 octahedral sites; and (4) BO_3 triangles between the Al-chains (Figure 1).

The crystallographic structure of dumortierite is

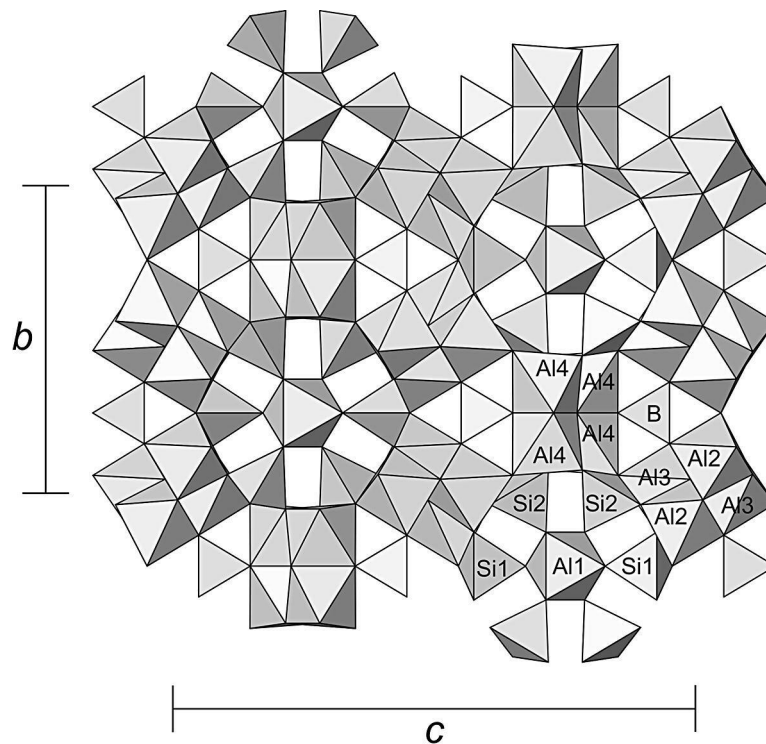


Figure 1. Dumortierite structure viewed along the a-axis (Groat et al., 2012).

orthorhombic, $Pnma$ (space group no. 62), with unit cell parameters of $a=4.69 \text{ \AA}$, $b=11.80 \text{ \AA}$, $c=20.19 \text{ \AA}$ (Groat et al., 2012). Common tetrahedrally-coordinated cation substitutes for Si are Al, As^{3+} and Sb^{3+} and the main octahedrally-coordinated cation substitutes for Al are Fe^{2+} , Fe^{3+} , Ti, Mg, Ta, Nb, with minor Ca, Mn and Sc. Minor amounts of P have also been reported (Grew, 2002; Evans et al., 2012, Groat et al., 2012). There is no substitution or vacancies at the B site in any natural dumortierite group minerals (Evans et al., 2012).

Magnesiumdumortierite contains up to 3.4 wt% MgO (Visser and Senior, 1991) and up to 4.4 wt% Fe_2O_3 (Claringbull and Hey, 1958). Ti content may rich up to 4.6 wt% (Huijsmans et al., 1982). Transformation of dumortierite to Ti-free magnesiumdumortierite is favoured at high pressure (Chopin et al., 1995). Magnesiumdumortierite has only been found in ultrahigh-pressure rocks of the western Alps.

In deep environments, boron can only be hosted in small amounts by white micas and sillimanite and in more significant amounts by dumortierite, tourmaline and datolite (Tornos et al., 2012). Dumortierite is sometimes unstable and locally associated with tourmaline. Spatially associated copper and gold prospects within this aluminosilicate-rich alteration zone is reported from the Louvicourt dumortierite-bearing schist (Taner, 1993). Dumortierite along with tourmaline are widespread in

magmatic-hydrothermal mineralized systems, occurring in breccias and veins related to copper, molybdenum and gold deposits (e.g., Island Copper Mine, British Columbia; Evans et al., 2012; Lincoln Hill, Nevada, and Louvicourt Mine, Quebec; Horn et al., 2014). Dumortierite geochemistry can be a valuable tool for constraining the source of boron and, by extension, the origin of fluids responsible for B-rich alteration in Cu-Au porphyry formation, since the current genetic discussion fluctuates between fluids derived from magmatic-hydrothermal systems and basinal brines related to marine evaporites. This study reports the first dumortierite compositional and FTIR data for Ali Javad porphyry Cu-Au deposit in the Sheivar Dagh area, NW Iran. Moreover, mineral chemistry and FTIR spectra of the samples have been compared with dumortierite samples of different origins worldwide.

Intrusion of the major Qaradagh and Sheivar Dagh plutons and numerous smaller intrusions in NW Iran caused development of extensive alteration zone and Cu-Mo-Au mineralization (Simmonds et al., 2017). These plutons with Cenozoic age are intruded the Cretaceous Cenozoic volcanic and volcano-sedimentary rocks (e.g., Simmonds and Moazzen, 2015; Simmonds et al., 2019). The Ali Javad Cu-Au porphyry deposit is one of the mineralizations associated with the Sheivar Dagh intrusion and the related alterations (Figure 2).

It is located in the East Azerbaijan province, NW Iran, and dumortierite was first reported from this deposit by Didon and Gemain (1976) and Kazempour et al. (2002). It appears in the advanced argillic and silicic alteration zones of this porphyry system as a result of late stage hydrothermal activities. We have studied the mineralogy of dumortierite of Ali Javad deposit using XRD, ICP-MS, EPMA and FTIR methods in order to constrain its physico-chemical conditions at the formation during late hydrothermal stage. The chemistry of dumortierite is used as a possible indicator of Cu-Au mineralization at this part of the porphyry copper metallogenic belt of Iran.

FIELD GEOLOGY AND DESCRIPTION OF DUMORTIERITE-BEARING ROCKS

The Ali Javad porphyry Cu-Au deposit is located in the general area of the Sheivar Dagh in NW Iran. The field geology of the Sheivar area is discussed in the 1:250,000 scaled geological map of Ahar (Babakhani et al., 1990). The Sheivar Dagh pluton has a granite to monzogranite

composition, which has caused contact metamorphism (Moazzen and Modjarrad, 2005) and vast hydrothermal alteration (Khaleghi et al., 2013) within the country rocks. However, new exploration diamond drillings and the obtained cores indicate the presence of younger stocks within the Sheivar plutonic complex in the Ali Javad area, cutting the main pluton, which are responsible for alteration and porphyry mineralization. This younger intrusive phase appears as dykes and apophyses in the area. The main pluton with quartz monzonite to monzogranite composition is emplaced at higher depth, and portrays coarse-grained granular texture, while the later magmatic phases of granite are emplaced at lower depth, which show porphyry texture. This feature is similar to other porphyry Cu deposits of NW Iran (Hassanpour and Moazzen, 2017; Simmonds et al., 2017).

The oldest rock units in the study area are Upper Cretaceous marl and sandstone, which are covered by Eocene rocks (Figure 2). The stratigraphic sequence at the Ali Javad, from older to the younger units are marl,

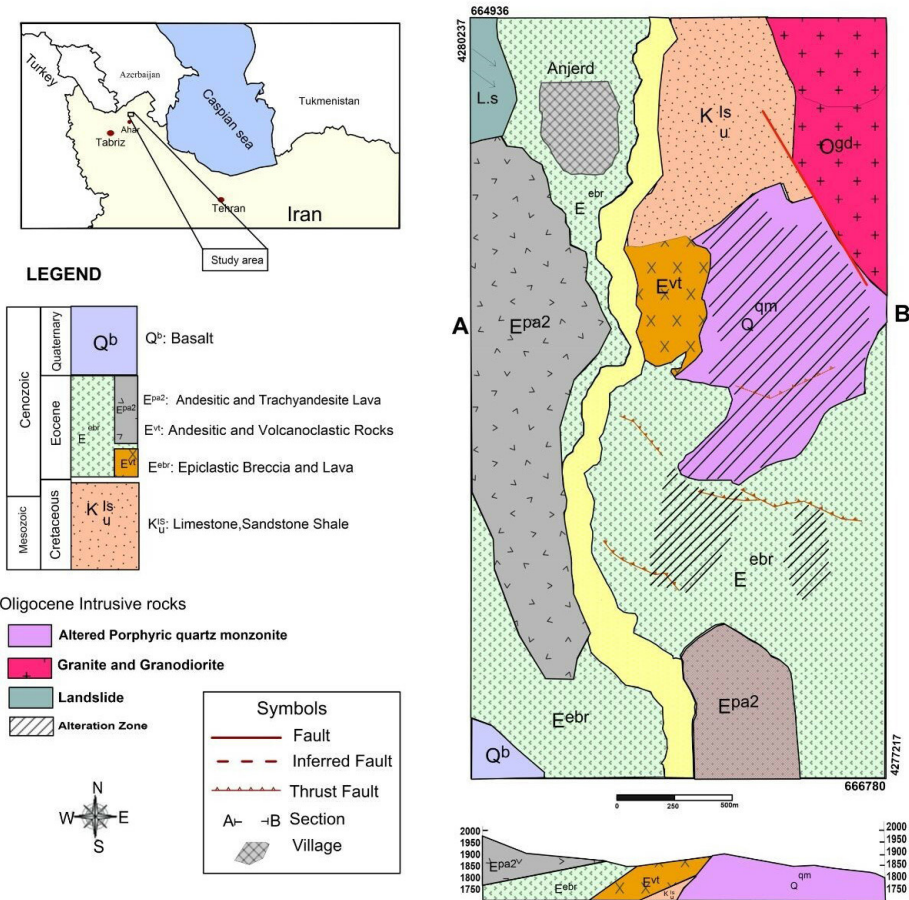


Figure 2. Simplified geological map of the study area.

sandstone, volcanic rocks, including trachy-basaltic andesite, trachyandesite-basalt and a succession of lava and tuff, including megaporphyritic andesite to trachy-andesite. Quaternary basalt and cover the older rocks (Figure 2). Intrusion of Oligocene plutonic rocks with predominant quartz monzonite to monzogranite composition into the Cretaceous and Eocene units has formed contact metamorphic rocks (Moazzen and Modjarrad, 2005) and skarn deposits (Mollaei et al., 2009). The main mineral deposits around the Sheivar pluton are Mazraeh and Anjerd skarns and Hajalibeig mineralized silicic veins. Upper Eocene-Oligocene magmatic activities were responsible for ore mineralization in the area (Bazin and Hubner, 1969). Quartz monzonitic stock in the area is characterized by the development of silicic veins and alteration zones similar to those from porphyry systems (Figure 3) (Khaleghi et al., 2013). The main alterations in the Ali Javad porphyry Cu-Au deposit are potassic, phyllic, propylitic, argillic and advanced argillic alterations (Figure 3). The development of alteration zones is more pronounced at the central part of the area and shows a NE-SW trend. The phyllic alteration corresponds to the megaporphyritic andesite unit, which is accompanied by stockwork structure and relatively high pyrite content (Khaleghi et al., 2013).

Dumortierite is found in diamond drill cores of the advanced argillic alteration zone (Figures 4 and 5). This mineral appears in samples collected at a depth of 170 meters which is accompanied by minerals such

as pyrophyllite, alunite, sericite, pyrite and copper minerals. Based on the field geology relations, this mineral is formed at the late stage of mineralization and by hydrothermal activity. It macroscopically appears with distinct blue color and as small patches or veins (Figure 6) and microscopically as fibrous or acicular crystal aggregates up to 1 mm long (Figure 7 a,b), occasionally showing spherulitic texture (Figure 7 c,d). Also it is disseminated among other minerals in some samples and is with variable colors from blue to violet and pink and strong pleochroic (bluish to pale blue) in thin sections. Dumortierite strongly pleochroic (bluish to pale blue) where it is locally associated with tourmaline (Fig 7 c,d). The accompanying minerals are either quartz or sericite along with opaque minerals or quartz and neo-formed biotite (Figure 7 e,f).

MATERIALS AND METHODS

Optically well characterized representative samples of dumortierite-bearing rocks were selected for mineralogical and geochemical studies. In two samples (surficial: no. DUMR_Alj 1 and core sample: no. DUMOR_Alj DH27_91 the depth of 91 meters), dumortierite was separated from the rock by hand picking under a binocular microscope in the University of Tabriz. XRD analysis was carried out on one separated sample (DUMOR_Alj DH27_91) in the Geological Survey of Iran, NW branch in Tabriz, using a SIEMENS D5000 X-Ray Diffraction

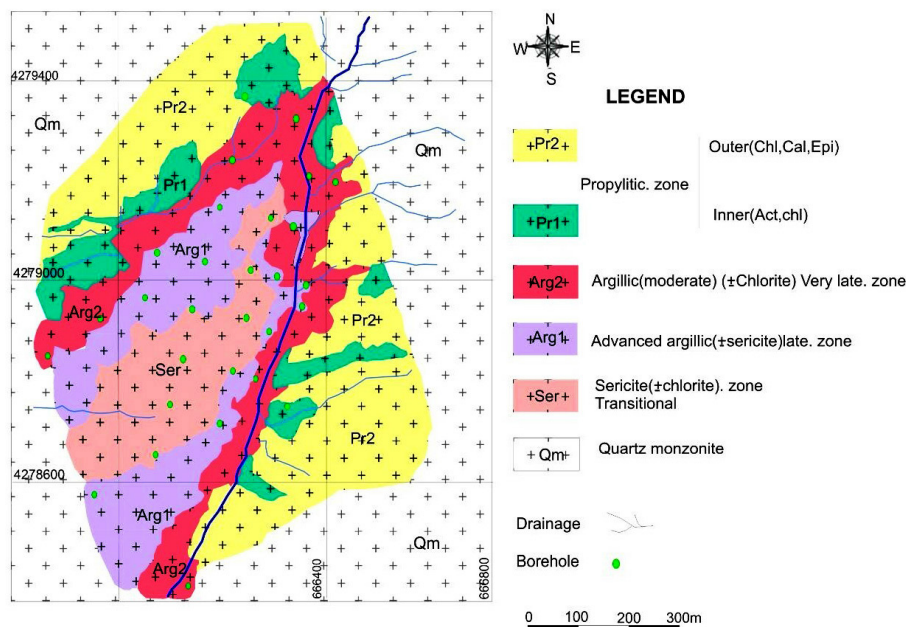


Figure 3. A general view of the distribution of alteration zones in the area.



Figure 4. A view of argillic alteration zone in the area, which appears as white patches.

Spectrometer with Ni-filtered Cu-K α source to identify the constituent minerals. The XRD data were recorded at 40 kV and 30 mA by counting 3 seconds at steps of $0.02^\circ 2\theta$, from 5 to $65^\circ 2\theta$.

Geochemical analyses were performed at Actlabs, Canada, by Fusion ICP (major oxides, Ba, Be, Sc, Sr, V, Y, Zr) and Fusion ICP-MS (Ag, As, Bi, Co, Cr, Cs, Cu, Ga, Ge, Hf, In, Nb, Ni, Mo, Pb, Rb, Sb, Sn, Ta, Th, Tl, U, W, Zn and REE) methods on the above-mentioned dumortierite separates samples. The known amount of sample was mixed with lithium metaborate and was fused on gas heater. The resulted beads were used for ICP-MS analyses after digestion in acid and necessary dilution. International standards were used for calibration. The uncertainty for the analysed minor and trace elements is better than $\pm 5\%$. Electron microprobe studies were done in Potsdam, Germany using a JEOL 8800 Superprobe, operated at 15 kV and 20 nA beam current and 2-10 mm beam diameter. Counting times were 10-30 seconds on peak and half-peak on background. Natural and synthetic samples were used for calibration. 14 spots of dumortierites were analyzed in this way. Infra-red spectroscopy analyses were done in the inorganic chemistry laboratory of Islamic Azad University, Tabriz branch. The sample was powdered in an agate mortar and then diluted in KBr and pressed to disk. FTIR spectra of the studied samples were recorded at room temperature by means of a Shimadzu 8400S spectrometer employing about 2 mg powder samples embedded in KBr pellets.

RESULTS AND DISCUSSION

X-ray diffraction pattern of the Ali Javad dumortierite reveals a relatively well crystallized structure, with the strong reflection at 5.91 Å and moderately strong reflections at 5.87 Å, 4.26 Å, 3.34 Å, 2.46 Å, and 2.12 Å (Figure 8). By the use of least-squares refinement, the calculated cell dimensions of dumortierite are $a = 11.77$ Å, $b = 20.21$ Å, $c = 4.71$ Å and $V = 1123.4$ Å³, respectively. This pattern is almost identical to the pattern of the standard dumortierite sample (Figure 8a). Thus, it is possible to discuss the nature of the studied dumortierite (e.g., Fe-Ti depleted) based on the XRD results (Sang et al., 1996; Choo and Kim, 2001).

According to the ICP-MS analysis data of two dumortierite separates (Table 1) 0.60 OH is considered in the dumortierite formula unit (Alexander et al., 1986; Platonov et al., 2000). The analyses indicate that the studied dumortierites are Mg-poor and of common Fe-Al dumortierite type. The Ali Javad samples also contain about 167 ppm Pb, 24 ppm Sb, 8 ppm Mo and 9 ppm Ga. An interesting result is the unusual occurrence of As, whose content reaches up to 400 ppm. The enrichment of some of the elements has been previously reported from other specimen. Dumortierite porphyroblast from Mozambique quartzites (high pressure conditions) is strongly zoned in Si, Al, Ti and Sb (Vaggelli et al., 2004). The Mozambique quartzites display unusual occurrence of Sb, with concentrations up to 5 wt% Sb₂O₃, representing a mineral with an intermediate composition between dumortierite and holtite (Ta,Sb)Al₆(SiO₄)₃BO₃(O,OH)₃.



Figure 5 Altered quartz monzonite unit in the Ali Javad valley. View to the West.

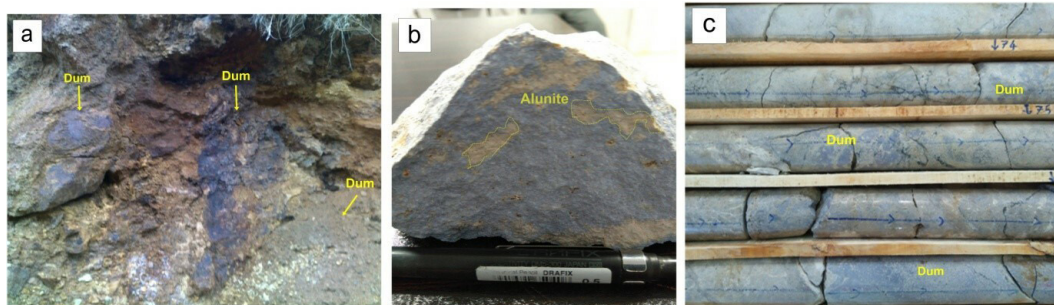


Figure 6. Surface and core samples containing dumortierite a) in porphyry dacite outcrop, b) in veins along with alunite (sample no. DUMR_Alj 1), c) core samples (BH41-75).

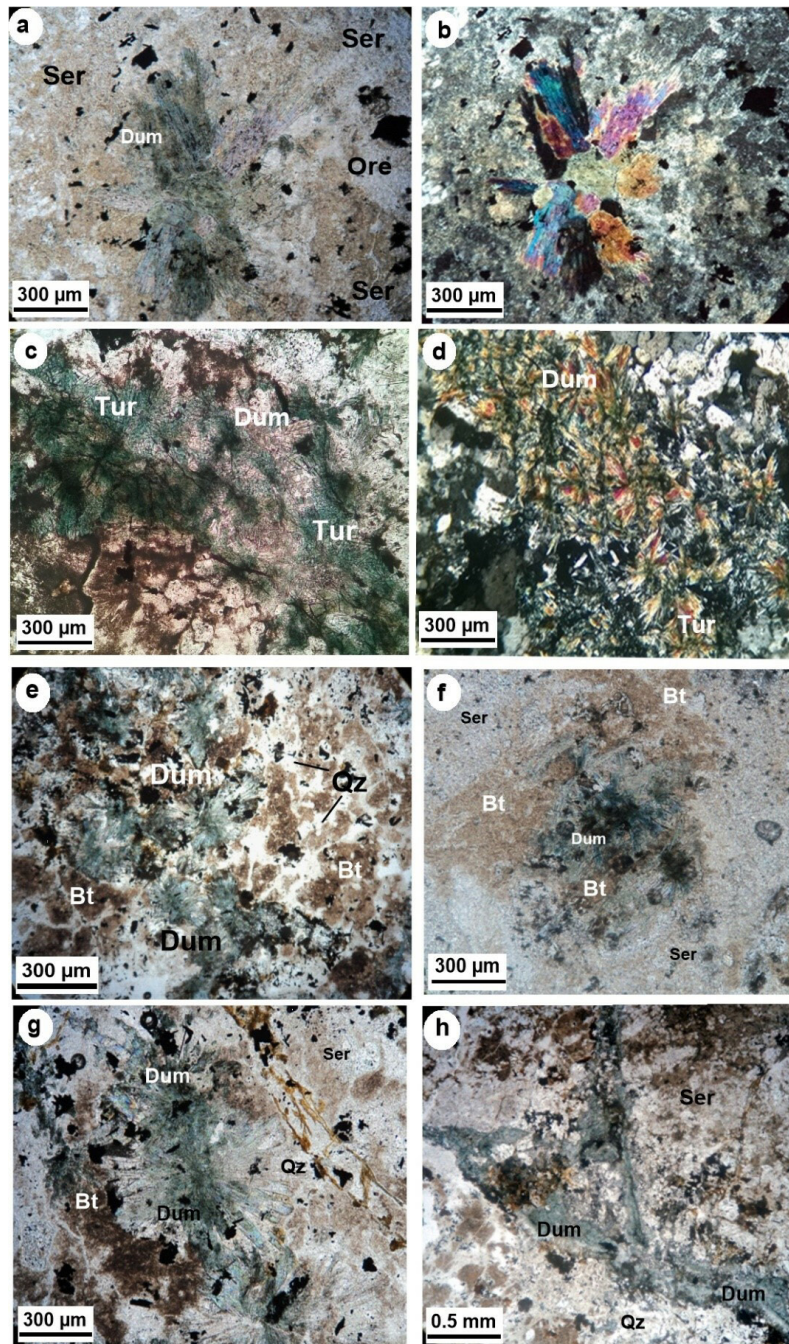


Figure 7. Dumortierite in advanced argillic to sericitic alteration zone. a, b) fibrous dumortierite in highly silicified rock along with quartz and sericite from core sample at the depth of 163m; PPL and XPL respectively. c, d) Spherulitic growth of dumortierite and tourmaline in veinlet from BH41 core sample at depth of 70m; PPL and XPL respectively. e, f) Concentration of dumortierite along with biotite and oxide phases in core sample from the depth of 157 m. g) dumortierite in core sample from depth of 40m. h) highly silicified rock along with ore and secondary iron hydroxides, dumortierite is formed as veinlet in the rock.

Dumortierite-group minerals commonly contain Ta, Nb, As and Sb, and locally, Bi, all of which represent solid solution with holtite-group minerals and szklaryite ($\square\text{Al}_6\text{BAs}^{3+}_3\text{O}_{15}$) (Pieczka et al., 2013).

Dumortierite crystals were analyzed by electron microprobe along a cross section for a total of 8 and 6 spots in the two selected samples. Table 2 presents electron microprobe analysis results of the studied dumortierites.

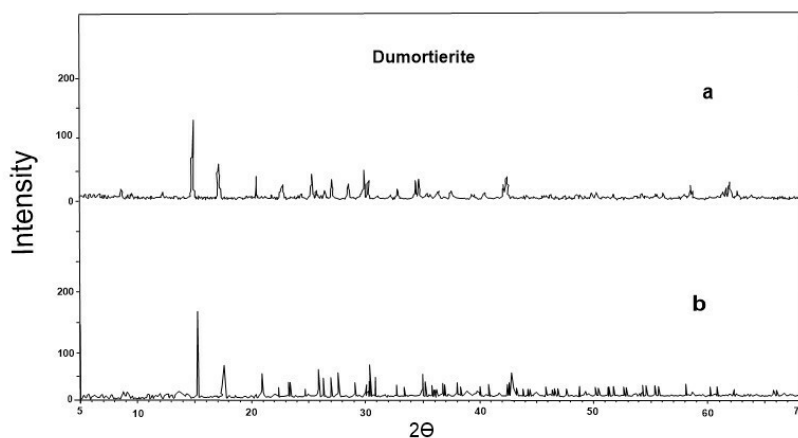


Figure 8. X-ray diffraction pattern for (a) dumortierite (RRUFF Database), (b) Ali Javad dumortierite sample (no. DUMR_Alj 1).

The Al_2O_3 content is between 61.03 and 61.24 wt%. The samples virtually lack MgO (0.03 wt%) and contain very low FeO (0.24 to 0.33 wt%). All Fe is considered as Fe^{2+} .

TiO_2 content varies from 1.17 to 1.25 wt%. There is a good correlation between the Ti content and the violet-blue pleochroism, as previously reported for other dumortierite samples (Vaggelli et al., 2004).

REE patterns of the analyzed dumortierite samples normalized to chondrite (Sun and McDonough, 1989; Thompson, 1982) show enrichment of large ionic lithophile (LILE) incompatible elements such as Th, Ba and Rb, whereas high field strength elements (HFSE) like Yb and Nb show lower concentrations (Figure 9). Enrichment of Th, Rb, Ba and depletion of Ti and Nb in the studied samples can be attributed to the inheritance from fluids of evolved subduction-related magmas (Foley et al., 1987; Wilson, 1990), therefore the observed features are consistent with a magmatic-hydrothermal origin.

In the FTIR spectrum, a large broad peak occurs, indicating hydroxyl stretching vibration (Figure 10). This shows that the hydroxyl group is loosely incorporated in the dumortierite structure. Boron presence in the three-fold coordination as part of a planar BO_3 group can be conceived from strong absorption peak. The FTIR spectra for the Ali Javad sample (no. DUMR_Alj 1) is comparable with FTIR spectra of samples from different origins at the range of $4000\text{--}400\text{ cm}^{-1}$. For comparison, the IR spectrum of two synthetic samples of low (no. B12) and high fluid pressures (no. P8a) (achieved by Werding and Schreyer, 1990), and a natural Fe-containing dumortierite of blue color from Madagascar is also shown (Figure 10c). There are no considerable differences, especially not in the spectra of our sample. The $\sim 3490\text{ cm}^{-1}$ band is present in all specimens. The distinct OH valency band at $\sim 3490\text{ cm}^{-1}$ (Werdning and Schreyer,

1983a) is broadened especially in sample B12, which is similar to Ali Javad spectrum. In this regard, the Ali Javad dumortierite contains more water and more Al (see Table 3). The strong BO_3 asymmetric valency band (Werdning and Schreyer, 1990) at $\sim 1385\text{ cm}^{-1}$ is very similar in all samples. The broadening of the $\gamma_3\text{-SiO}_4$ band at about 1000 cm^{-1} and the different intensity of the band at 850 cm^{-1} , possibly $\gamma_3\text{-AlO}_4$, are distinctly evident.

CRYSTAL CHEMISTRY OF ALI JAVAD DUMORTIERITE

Dumortierite has been usually considered as an anhydrous mineral with formula of $\text{Al}_7\text{BSi}_3\text{O}_{18}$, but spectroscopic analysis revealed the presence of hydroxyl groups (Moore and Araki, 1978; Alexander et al., 1986; Werding and Schreyer, 1990). Moore and Araki (1978), Hemingway et al. (1990), and Visser and Senior (1991) proposed 0.75 OH per formula unit, though Alexander et al. (1986) and Platonov et al. (2000) suggested different hydroxyl contents, e.g. 0.6 OH. The total amount of OH varies not only with the number of octahedral vacancies but also with the divalent ions such as Mg, Ca, Fe^{2+} and tetravalent substituent for octahedral Al and trivalent substituent for tetrahedral Si (Alexander et al., 1986; Werding and Schreyer, 1990). The Ali Javad dumortierite contains negligible Fe, Mg and Ti. For comparison, magnesioidumortierites commonly contain these elements up to a few percent (Visser and Senior, 1991). Our sample may contain some hydroxyl, as shown by IR spectroscopy. Structural formula of dumortierite is recalculated as $(\text{Al}_{7.51}\text{Fe}_{0.03})_{\Sigma 7.54}\text{Si}_{3.25}\text{BO}_{17.62}$. The fact that Al is slightly excessive per formula unit can be explained by the common association with other Al-rich minerals such as alunite, dickite, pyrophyllite and tourmaline in the Ali Javad deposit.

Due to analytical limitations for boron by EPMA, B

Table 1. Results from ICP-MS analyses of the dumortierite in Ali Javad samples.

Analyte Symbol	SiO ₂	Al ₂ O ₃	FeO	MnO	MgO	CaO	Na ₂ O	K ₂ O	TiO ₂	P ₂ O ₅	LOI	Total
Unit Symbol	%	%	%	%	%	%	%	%	%	%	%	%
Detection Limit	0.01	0.01	0.01	0.001	0.01	0.01	0.01	0.01	0.001	0.01		0.01
DUMOR_Alj DH27_91	70.03	20.56	1.94	0.001	0.13	0.11	0.06	0.09	1.123	0.29	4.84	98.77
DUMOR_Alj 1	69.27	21.17	2.27	0.001	0.12	0.1	0.08	0.07	1.442	0.26	4.7	98.54
Analyte Symbol	Sc	Be	V	Cr	Co	Fe	Al	Mg	Ni	Cu	Zn	Ga
Unit Symbol	ppm	ppm	ppm	ppm	ppm	%	%	%	ppm	ppm	ppm	ppm
Detection Limit	1	1	5	20	1				20	10	30	1
DUMOR_Alj DH27_91	18	1	207	< 20	19	1.5	5.34	0.07	< 20	20	< 30	8
DUMOR_Alj 1	19	1	198	< 20	18	1.76	5.5	0.073	< 20	21	< 30	9
Analyte Symbol	Ge	As	Rb	Sr	Y	Zr	Nb	Mo	Ag	In	Sn	Sb
Unit Symbol	ppm	ppm	ppm	ppm	ppm	ppm	ppm	ppm	ppm	ppm	ppm	ppm
Detection Limit	1	5	2	2	2	4	1	2	0.5	0.2	1	0.5
DUMOR_Alj DH27_91	4	400	< 2	865	7	114	6	7	< 0.5	0.3	21	23.6
DUMOR_Alj 1	3	395	< 2	703	6	133	5	8	< 0.5	0.2	19	24.1
Analyte Symbol	Cs	Ba	La	Ce	Pr	Nd	Sm	Eu	Gd	Tb	Dy	Ho
Unit Symbol	ppm	ppm	ppm	ppm	ppm	ppm	ppm	ppm	ppm	ppm	ppm	ppm
Detection Limit	0.5	3	0.1	0.1	0.05	0.1	0.1	0.05	0.1	0.1	0.1	0.1
DUMOR_Alj DH27_91	< 0.5	225	11.6	23.4	2.85	11.6	2.3	0.59	1.6	0.2	1.2	0.2
DUMOR_Alj 1	< 0.5	233	10.8	25.1	2.85	10.9	2.4	0.63	1.7	0.2	1.1	0.3
Analyte Symbol	Er	Tm	Yb	Lu	Hf	Ta	W	Tl	Pb	Bi	Th	U
Unit Symbol	ppm	ppm	ppm	ppm	ppm	ppm	ppm	ppm	ppm	ppm	ppm	ppm
Detection Limit	0.1	0.05	0.1	0.04	0.2	0.1	1	0.1	5	0.4	0.1	0.1
DUMOR_Alj DH27_91	0.8	0.16	1.2	0.22	2.7	0.4	4	0.2	167	0.9	4.5	1.2
DUMOR_Alj 1	0.7	0.18	1	0.21	2.8	0.5	6	0.1	156	0.8	4.3	1.3

Analysis Method: Fusion ICP for Major Elements/Fusion ICP-MS for Trace Elements.

Table 2. Microprobe analyses of dumortierite samples.

	DUMOR_Alj DH27_91 n=8		DUMOR_Alj 1 n=6		Samples Average composition
	Avg.	Std. Dev.	Avg.	Std. Dev.	
SiO ₂	31.15	0.35	31.22	0.28	31.18
TiO ₂	1.17	0.22	1.25	0.13	1.21
Al ₂ O ₃	61.03	0.37	61.24	0.37	61.13
B ₂ O ₃ *	5.78	0.43	5.33	0.54	5.56
Cr ₂ O ₃	0.003	0.001	0.002	0.001	0.002
MgO	0.03	0.028	0.03	0.01	0.03
CaO	0	0.00	0	0.00	0.000
MnO	0.001	0.001	0.002	0.001	0.001
FeO	0.24	0.07	0.33	0.06	0.28
Fe ₂ O ₃	0.27	-	0.37	-	0.31
Na ₂ O	0.001	0.001	0.003	0.002	0.002
K ₂ O	0.004	0.003	0.003	0.002	0.003
H ₂ O*	0.6	0.00	0.6	0.00	0.6
Total (wt.%)	100.28	0.15	100.4	0.13	100.30
Si	3.256	0.0000	3.250	0.0000	3.253
Ti	0.092	0.0000	0.098	0.0000	0.095
Al	7.518	0.0000	7.514	0.0000	7.516
B*	0.959	0.000	0.887	0.000	0.924
Cr	0.000	0.0000	0.000	0.0000	0.000
Fe ³⁺	0.021	0.0000	0.028	0.0000	0.034
Mg	0.005	0.0000	0.000	0.0000	0.005
Mn	0.000	0.0000	0.000	0.0000	0.000
Ca	0.000	0.0000	0.000	0.0000	0.000
Na	0.000	0.0000	0.000	0.0000	0.000
K	0.000	0.0000	0.000	0.0000	0.000
Sum cations	10.981	0.000	10.976	0.000	10.991
OH*	0.38	0.00	0.38	0.00	0.38

* B₂O₃ and H₂O content calculated on the basis of ideal stoichiometry. See text for assumptions concerning boron and hydroxyl.

was calculated based on the assumption of 1 B cation per formula unit, assuming full occupancy of the boron site which makes it possible to calculate the weight % of B₂O₃ required (Alexander et al., 1986; Werding and Schreyer, 1990; Visser and Senior, 1991; Platonov et al., 2000). The formula was calculated based on 18 oxygen atoms (17.40 oxygen atoms and 0.60 OH, after Moore and Araki, 1978 and Werding and Schreyer, 1990). The

formula derived from the average electron-microprobe composition of Ali Javad sample is (Al_{7.51}Fe_{0.03})_{Σ7.54}Si_{3.25}BO_{17.62}. The formula from the crystal-structure refinement is (Al_{6.77}□_{0.23})_{Σ7}Si₃BO₁₈, which must include OH for charge-balance considerations and becomes (Al_{6.77}□_{0.23})_{Σ7}Si₃B(O_{17.62}OH_{0.38})_{Σ18}. In the dumortierite structure, OH is considered to occur in the hexagonal channel at the O2 and O7 positions (Moore and Araki,

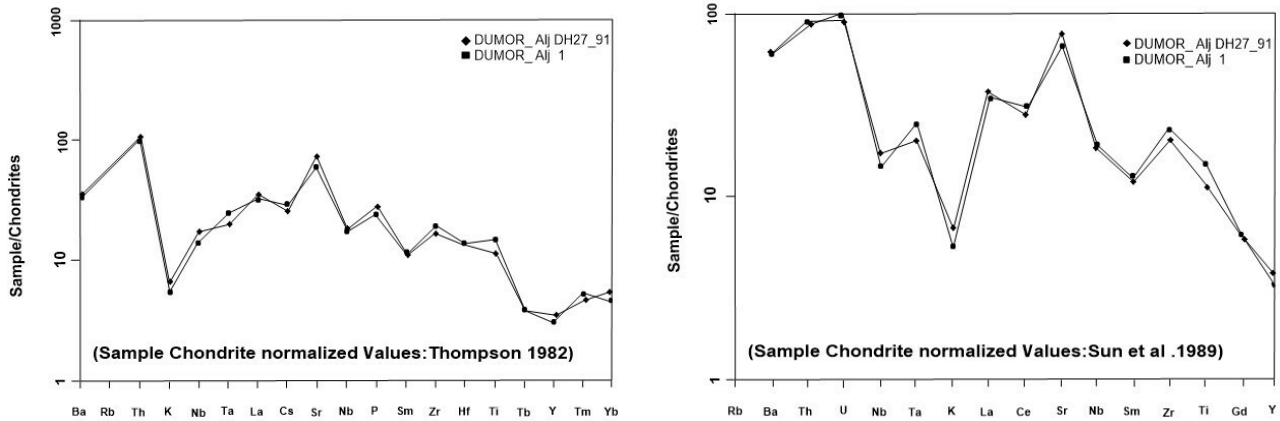


Figure 9. Spider diagram for the analyzed dumortierite samples. Normalization values from Thompson (1982) and Sun and McDonough (1989).

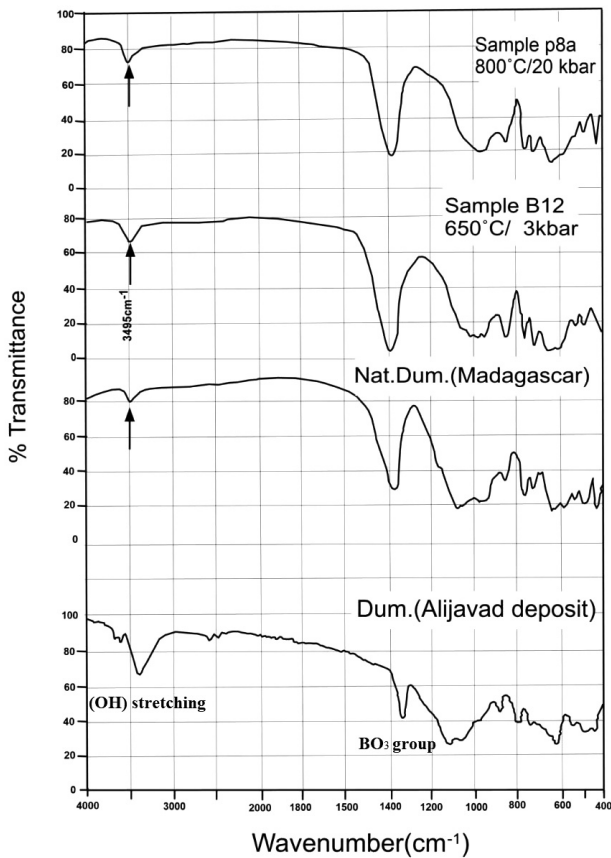


Figure 10. FTIR spectrums of some dumortierite samples from different origins, provided for comparison. a,b) Infrared spectra of two synthetic (p8a and B12) in the 4000-400 cm^{-1} region (Fuchs et al., 2005). c) One natural sample of dumortierite from Madagascar (Werding et al., 1990). d) FTIR spectra of the Ali Javad dumortierite.

1978; Alexander et al., 1986; Werding and Schreyer, 1990; Cempírek and Novák, 2005; Fuchs et al., 2005), and at the four coordinated O10 site (Chopin et al., 1995). In Table 3, results of average microprobe analysis of Ali Javad dumortierite have been compared with samples from different origins. Results show important variations of Al_2O_3 and SiO_2 content in samples of different localities. High P_2O_5 contents ($\sim 0.5\%$) are observed in the Louvicourt dumortierite. The As_2O_5 average content reaches 0.282% in the Lincoln Hill specimens. Sb_2O_3 content reaches 0.34 % in the Lincoln Hill dumortierite, but is far below the average value (2.46 wt%) of the Mozambique dumortierite (with a maximum up to 4.50%, Vaggelli et al., 2004). TiO_2 content varies from 0.47 up to 1.82%, far below the 3.15 wt% TiO_2 of the dumortierite in the Mozambique metamorphic quartzite. Dumortierite porphyroblast from the Mozambique quartzites displays high contents of heavy elements (i.e. Sb and Ti), representing a mineral with an intermediate composition between dumortierite and holtite ($\text{Ta,Sb Al}_6(\text{SiO}_4)_3\text{BO}_3(\text{O,OH})_3$) (Vaggelli et al., 2004).

It is known that Fe and Ti are responsible for the pink and blue colour of dumortierite, depending on the relative importance of $\text{Fe}^{2+}\text{-Fe}^{3+}$ and $\text{Fe}^{2+}\text{-Ti}^{4+}$ charge transfers, respectively (Alexander et al., 1986). According to the classification of colors by the $\text{Fe}/(\text{Fe}+\text{Ti})$ ratio in dumortierite (Alexander et al., 1986), the chemical composition of the Ali Javad dumortierite lies in the blue color region. The color and pleochroism of dark blue, red and violet dumortierite is caused by excitation of $\text{Fe}^{2+}\text{-Ti}^{4+}$ charge transfer. These colors are seen in samples from Madagascar and Mozambique. This is also in accordance with the compositional findings by Alexander et al. (1986) in dumortierite samples.

Table 3. Comparison of average electron microprobe compositions of the Ali Javad dumortierite with other samples from different origins (in weight %).

Sample	Ali Javad (Iran)	Lincoln Hill (USA)	Miryang (Korea)	Louvicourt (Canada)	Weißenkirchen (Austria)	Girola (India)	Madagascar	Mozambique
SiO ₂	31.18	30.73	29.31	29.6	30.21	30.94	30.19	29.51
Al ₂ O ₃	61.13	60.57	57.68	59.2	59.22	59.82	59.9	57.09
MgO	0.03	0.03	0.49	0.68	0.84	0.32	0.001	0.275
Sb ₂ O ₃	n.a.	0.34	n.a.	0.008	n.a.	0	0.109	2.46
FeO	0.28	0.24	0.31	0.056	0.33	0.15	0.38	0.195
K ₂ O	0.003	-	0.0	n.a.	0.01	0.03	n.a.	-
Na ₂ O	0.002	0.009	0.0	0.016	0.01	0.02	0.012	-
TiO ₂	1.21	0.55	0.0	1.31	1.74	1.82	0.47	3.15
As ₂ O ₅	n.a.	0.282	n.a.	0.066	n.a.	n.a.	n.a.	-
MnO	0.001	n.a.	0.0	n.a.	0.01	0.03	n.a.	-
P ₂ O ₅	n.a.	0.059	n.a.	0.49	n.a.	0.01	0.05	-
Source Dumortierite	Hydrothermal porphyry gold-bearing	Low sulfide gold-bearing veins (Horn et al., 2014)	Clay deposit from granite Altered (Choo and Kim, 2001)	Hydrothermal alteration and later metamorphism (Fuchs et al., 2015)	Pegmatites related to metamorphic rocks (Fuchs et al., 2005)	Metamorphic schists (Meshram et al., 2012)	Regional metamorphism (Horn et al., 2014)	High Pressure Quartzite (Vaggelli et al., 2004)

Comparing the data of Table 3 and considering all the above-mentioned discussions, it is clear that high-pressure dumortierites are always less aluminous than those formed at low pressures. Dumortierite has commonly slight excess of Al per formula unit, for example in Miryang deposit, which is presumably due to the crystallization of Al-rich phases composed of diaspore, dickite, pyrophyllite and tourmaline (Choo and Kim, 2001). Furthermore, the compositions of dumortierite crystals from gold-bearing hydrothermal systems are very similar, as it is expectable, and may therefore reflect similar *PT* conditions and fluids during crystallization in these deposits (Table 3).

Considering the vast alterations in the area and sulphide mineralization, it seems that boron for dumortierite crystallization is originated from the Ali Javad intrusive stock. The absence of boron-bearing evaporitic minerals in the country rocks further confirms this deduction. Boron as an incompatible element was not able to enter the silicate minerals crystallized at the early stages of magma crystallization. This would cause boron accumulation in the late stage fluids, which are responsible for the vast alterations in the area. This has also crystallized dumortierite in the altered rocks. By decreasing of Fe, Na, Sr, Mg and Ca concentration in the late stage hydrothermal

fluids due to development of alteration zones and prior to boron addition, tourmaline will not crystallize in the system and dumortierite will be formed instead. The breakdown of boron-bearing precursor such as tourmaline (Choo and Kim, 2001) could have supplied the boron for the dumortierite formation, as suggested by local association of dumortierite and tourmaline (Figure 7 c,d).

Development of advanced argillic alteration zone, or "lithocap" is common at shallow levels above the porphyry Cu-Au deposits (e.g., in Lepanto-Far Southeast, Philippines; Maricunga, Chile; Oyu Tolgoi, Mongolia). These lithocaps are considered as exploration guides, since they can be formed spatially adjacent to the porphyry Cu systems (Mavrogenatos et al., 2018). Many lithocaps are vertically zoned, from quartz-pyrophyllite at depth to predominant quartz-alunite at shallower levels, where the responsible fluid was cooler and more acidic (Sillitoe, 2010). The key minerals in the lithocaps are pyrophyllite, kaolinite, alunite and dickite. These mineral assemblages are usually associated with silica and sometimes include diaspore, andalusite, corundum, topaz and dumortierite. The principal borosilicate mineral in lithocaps is dumortierite rather than tourmaline (Sillitoe, 2010).

The presence of dumortierite in the advanced argillic

alteration lithocaps has been reported from a number of gold-rich porphyry copper systems and prospects worldwide, including the Island Copper deposit, British Columbia in Canada (Panteleyev et al., 1993), and Elshitsa in Bulgaria (Kouzmanov et al., 2009), the Oyu Tolgoi in Mongolia (Khashgerel et al., 2008) and Saindak in Pakistan (Perello et al., 2008). In Iran, the best-known and the only example of dumortierite occurrence in a lithocap above a porphyry system is in the Sarsefidal district near Kashmar, NE Iran (Karimpour, 2005).

It is postulated that the development of dumortierite is a mineralogical expression of the association of acid metasomatism with precious metal and base-metal mineralization (Taner, 1993).

Assemblages of peraluminous minerals are known to be spatially associated with some gold and base metals deposits. In two examples of Chetwynd mine in southwestern Newfoundland and the Big Bell mine in Western Australia (Thompson et al., 1996), the gold deposit contains a dumortierite-bearing aluminosilicate horizon. As another group of examples, the sericite-rich schist horizon (ore-bearing felsic unit) of both the Doyon, Bousquet and LaRonde (formerly Dumagami mine) gold deposits contains dumortierite (Taner, 1993).

CONCLUSIONS

Dumortierite was found in diamond drill cores of the Ali Javad porphyry Cu-Au deposit, mainly within the advanced argillic alteration zone. Since this mineral is found down to 170 m, it can be used as an indicator mineral within the deposit cap for prospecting other similar gold-rich porphyry deposits. Low concentration of elements required for tourmaline crystallization in the alteration zone and in the hydrothermal fluids favored dumortierite crystallization instead of tourmaline in the study area. As the Ali Javad intrusive stock was crystallized, the large ions accumulated within the late stage hydrothermal fluids. This boron-bearing fluid invaded the porphyry mineralization host rocks and crystallized dumortierite. Given the absence of boron isotope data on Ali Javad deposit, that could have allowed comparison with other similar porphyry systems and determination of the boron derivation from magmatic/basement or marine evaporitic origins, data obtained in this study open up the possibility of using dumortierite chemistry as a tool for geothermobarometry of Ali Javad hydrothermal system.

ACKNOWLEDGEMENTS

We would like to thank Research and Technology deputy of Islamic Azad University of Tabriz for supporting this research financially and Mehr Asl Company. Prof. M. Moazzen is acknowledged for his helps. The valuable comments of two reviewers of the journal improved the manuscript. We appreciate

all help and support by Prof. Ballirano, the chief editor of the journal.

REFERENCES

- Alexander V.D., Griffen D.T., Martin T.J., 1986. Crystal chemistry of some Fe- and Ti-poor dumortierites. *American Mineralogist* 71, 786-794.
- Babakhani A.S., Lescuyah C., L Rio R., 1990. Description of Ahar Quadrilateral Geology Map. Geological Survey of Iran, 123 pp.
- Bazin D. and Hübner H., 1969. Copper Deposits in Iran. Geological Survey of Iran, Tehran, 232 pp.
- Beukes G.J., Slabbert M.J., de Bruijn H., Botha B.J.V., Schoch A.E., 1987. Ti dumortierite from Keimoes area, Namaqua mobile belt, South Africa. *Neues Jahrbuch für Mineralogie Abhandlungen* 157, 303-318.
- Black P.M., 1973. Dumortierite from Karikari peninsula: a first record in New Zealand. *Mineralogical Magazine* 39, 245.
- Cempirek J. and Novák M., 2006. Mineralogy of dumortierite-bearing abyssal pegmatites at Starkoč and Běstvína, Kutná Hora Crystalline Complex. *Journal of the Czech Geological Society* 51, 259-270.
- Choo C.O. and Kim J.J., 2001. Mineralogical studies of dumortierite from the Miryang clay deposit, Korea. *Geosciences Journal* 5, 273-279.
- Chopin C., Ferraris G., Ivaldi G., Schertl H.P., Schreyer W., Compagnoni R., Davidson C., Davis A.M., 1995. Magnesiodumortierite, a new mineral from very-high-pressure rocks (western Alps). II. Crystal chemistry and petrological significance. *European Journal of Mineralogy* 7, 525-535.
- Claringbull G.F. and Hey M.H., 1958. New data for dumortierite. *Mineralogical Magazine* 31, 901-907.
- Didon J. and Gemain Y.M., 1976. Le Sabalan, volcan plio-quaternaire de l'Azerbaïdjan oriental (Iran): étude géologique et pétro-graphique de l'édifice et de son environnement régional. Unpubl. PhD Thesis, Université Scientifique et Médicale de Grenoble France, 1-166.
- Evans R.J., Fyfe C.A., Groat L.A., Lam A.E., 2012. MAS NMR measurements and ab initio calculations of the ²⁹Si chemical shifts in dumortierite and holtite. *American Mineralogist* 97, 329-340.
- Foit F.F. Jr., Fuchs Y., Myers P.E., 1989. Chemistry of alkali deficient schorls from two tourmaline-dumortierite deposits. *American Mineralogist* 74, 1317-1324.
- Foley S.S., Venurelli G., Green D.H., Toscani L., 1987. The ultrapotassic rocks: Characteristics, classification and constraints for petrogenetic models. *Earth Science Reviews* 24, 81.
- Fuchs Y., Ertl A., Hughes J.M., Prowatke S., Brandstatter F., Schuster R., 2005. Dumortierite from the Gföhl unit, Lower Austria: chemistry, structure, and infra-red spectroscopy. *European Journal of Mineralogy* 17, 173-183.

- Golovastikov N.I., 1965. The crystal structure of dumortierite. *Soviet Physics-Doklady* 10, 493-495.
- Groat L.A., Evans R.J., Grew E.S., Pieczka, A., 2012. Crystal chemistry of As and Sb-bearing dumortierite. *The Canadian Mineralogist* 50, 855872.
- Hassanpour Sh. and Moazzen M., 2017. Geochronological Constraints on the Haftcheshmeh Porphyry Cu-Mo-Au Ore Deposit, Central Qaradagh Batholith, Arasbaran Metallogenic Belt, Northwest Iran. *Acta Geologica Sinica* 91, 2109-2125.
- Hemingway B.S., Anovitz L.M., Robie R.A., McGee, J.J., 1990. The thermodynamic properties of dumortierite $\text{Si}_3\text{B}[\text{Al}_{6.75}\square_{0.25}\text{O}_{17.25}(\text{OH})_{0.75}]$. *American Mineralogist* 75, 1370-1375.
- Henry D.J. and Dutrow B.L., 1996. Metamorphic tourmaline and its petrologic applications. In: Grew, E.S. and Anovitz, L.M. (Eds.): *Reviews in Mineralogy*, 33: Boron Mineralogy, Petrology and Geochemistry. Mineralogical Society of America, 500-555.
- Horn A.H., Fuchs Y., Carvalho Neves S.D., Balan E., Linares J., 2014. The occurrence of dumortierite in the Espinhaco Range, Minas Gerais, Brazil, and its mineralogical-crystallographic comparison with other specimen. *Revista Espinhaco* 3, 4-14.
- Huijsmans J.P.P., Barton M., van Bergen M.J., 1982. A pegmatite containing Fe-rich grandidierite, Ti-rich dumortierite and tourmaline from the Precambrian, high-grade metamorphic complex of Rogaland, SW Norway. *Neues Jahrbuch für Mineralogie Abhandlungen* 143, 249-261.
- Karimpour M.H., 2005. Petrology, mineralization and geochemistry of the Sarsefidal prospecting area (Kashmar, Khorasane Razavi). *Quarterly Shahid Chamran University Journal of Science, New Series*, 14.
- Kazempour E., Karimzadeh A., Malek Ghasemi F., 2002. The Occurrence of dumortierite mineral in the area of Ali Javad, northwest of Ahar. *Conference Proceeding of the Iranian Mineralogy and Crystallization Society, Yazd, 11th Iranian Conference on Crystallography and Mineralogy, Yazd University*, 151. (in Persian)
- Kerr P.F. and Jenney P., 1935. The dumortierite-andalusite mineralization at Oreana, Nevada. *Economic Geology* 30, 287-300.
- Khaleghi F., Hajalilou B., Shokohi H., 2013. Introduction of Ali Javad gold-rich porphyry Copper deposit, Anjerd, NW Ahar: *Proceedings of the 8th Geological Conference of Payame Noor University, Kerman*. (in Persian)
- Khashgerel B.E., Kavalieris I., Hayashi K.I., 2008. Mineralogy, textures, and whole-rock geochemistry of advanced argillic alteration: Hugo Dummett porphyry Cu-Au deposit, Oyu Tolgoi mineral district, Mongolia. *Mineralium Deposita* 43, 913.
- Kouzmanov K., Moritz R., von Quadt A., Chiaradia M., Peytcheva I., Fontignie D., Bogdanov K., 2009. Late Cretaceous Porphyry Cu and epithermal Cu-Au association in the Southern Panagyurishte District, Bulgaria: the paired Vlaykov Vruh and Elshitsa deposits. *Mineralium Deposita* 44, 611-646.
- Mavrogenatos C., Voudouris P., Spry P.G., Melfos V., Klemme S., Berndt J., Zaccarini F., 2018. Mineralogical Study of the Advanced Argillic Alteration Zone at the Konos Hill Mo-Cu-Re-Au Porphyry Prospect, NE Greece. *Minerals* 8, 479.
- Meshram R.R. and Ingle K.B., 2012. Mineralogy and origin of Dumortierite from Girola Area, Bhandara District, Eastern Maharashtra. *Journal Geological society of India* 79, 181-188.
- Moazzen M. and Modjarrad M., 2005. Contact metamorphism and crystal size distribution studies in the Sheivar aureole, NW Iran. *Geological Journal* 40, 499-517.
- Mollaei H., Yaghubpur A., Attar R.S., 2009. Geology and geochemistry of skarn deposits in the northern part of Ahar batholith, East Azarbaijan, NW Iran. *Iranian Journal of Earth Science* 1, 15-34.
- Moore P.B. and Araki T., 1978. Dumortierite, $\text{Si}_3\text{B}[\text{Al}_{6.75-0.25}\text{O}_{17.25}(\text{OH})_{0.75}]$: a detailed structure analysis. *Neues Jahrbuch für Mineralogie Abhandlungen* 132, 231-241.
- Panteleyev A. and Koyanagi V.M., 1993. Advanced Argillic Alteration in Bonanza Volcanic Rocks, Northern Vancouver Island-Transitions Between Porphyry Copper and Epithermal Environments (92L/12). In *Geological Fieldwork*.
- Perelló J., Raziq A., Schloderer J., 2008. The Chagai porphyry copper belt, Baluchistan province, Pakistan. *Economic Geology* 103, 1583-1612.
- Pieczka A., Evans R.J., Grew E.S., Groat L.A., Ma C., Rossman G.R., 2013. The dumortierite supergroup. I. A new nomenclature for the dumortierite and holtite groups. *Mineralogical Magazine* 77, 2825-2839.
- Sabzehei M., 1971. Dumortierite from Iran: a first record. *Mineralogical Magazine* 38, 526-527.
- Sang K.N., Chung W.W., Lee Y.J., 1996. Hydrothermal system of diaspore-dumortierite minerals from Korea. *Economic and Environmental Geology* 29, 439-446. (in Korean with English abstract)
- Schreyer W., Abraham K., Behr H.J., 1975. Sapphirine and associated minerals from kornerupine rock of Waldheim, Saxony. *Neues Jahrbuch für Mineralogie Abhandlungen*, 126, 1-27.
- Sillitoe R.H., 2010. Porphyry copper systems. *Economic Geology* 105, 3-41.
- Simmonds V. and Moazzen M., 2015. Re-Os dating of molybdenites from Oligocene Cu-Mo-Au mineralized veins in the Qrachilar area, Qaradagh batholith (northwest Iran): implications for understanding Cenozoic mineralization in South Armenia, Nakhchivan and Iran. *International Geology Review*, 57, 290-304.
- Simmonds V., Moazzen M., Mathur R., 2017. the timing of porphyry mineralization in northwest Iran in relation to Lesser Caucasus and Central Iran; Re-Os age data for Sungun porphyry Cu-Mo deposit. *International Geology Review*, 59, 1561-1574.

- Simmonds V., Moazzen M., Selby D., 2019. U-Pb zircon and Re-Os molybdenite age of the Siah Kamar porphyry molybdenite deposit, NW Iran. *International Geology Review*. doi: 10.1080/00206814.2018.1561334.
- Sun S.S. and McDonough W.F., 1989. Chemical and isotopic systematics of oceanic basalts: implications for mantle composition and processes. In: *Magmatism in the Ocean Basins* (Eds.): A.D. Saunders and M.J. Norry. The Geological Society 42, 313-345.
- Takahata H. and Uchiyama K., 1985. Dumortierite bearing argillaceous gneisses from the Abukuma metamorphic terrain, Northeast Japan. *Journal of the Faculty of Science, Hokkaido University*, 465-481.
- Taner M.F., 1993. Gold abundance and an aluminosilicate-rich alteration zone in the Val D'Or mining district, abitibi, Quebec: Examples of the fossil geothermal fields. *Ore Geology Reviews* 8, 451-475.
- Thompson A.J.B. and Thompson J.F.H., 1996. *Atlas of alteration: A field and petrographic guide to hydrothermal alteration minerals*. Geological Association of Canada, Mineral Deposits Division, 119 pp.
- Thompson R.N., 1982. British Tertiary province. *Scottish Journal of Geology* 18, 49-107.
- Tornos F., Wiedenbeck M., Velasco F., 2012. The boron isotope geochemistry of tourmaline-rich alteration in the IOCG systems of northern Chile: implications for a magmatic-hydrothermal origin. *Mineralium Deposita* 47, 483-499.
- Vaggelli G., Olmi F., Massi M., Giuntini L., Fedi M., Fiora L., Cossio R., Borghi A., 2004. Chemical Investigation of Coloured Minerals in Natural Stones of Commercial Interest. *Microchimica Acta* 145, 249-254.
- Visser D. and Senior A., 1991. Mg-rich dumortierite in cordierite orthoamphibole-bearing rocks from the high-grade Bamble Sector, south Norway. *Mineralogical Magazine* 55, 563-577.
- Vrána S., 1979. A polymetamorphic assemblage of grandidierite, kornrupine, Ti-rich dumortierite, tourmaline, sillimanite and garnet. *Neues Jahrbuch für Mineralogie Monatshefte* 1979, 22-33.
- Werdning G. and Schreyer, W., 1983a. High pressure synthesis of dumortierite. *Terra cognita* 3, 165 (EUG Abstract).
- Werdning G. and Schreyer W., 1990. Synthetic dumortierite: its PTX-dependent compositional variations in the system Al_2O_3 - B_2O_3 - SiO_2 - H_2O . *Contributions to Mineralogy and Petrology* 105, 11-24.
- Wilson M., 1990. *Igneous Petrogenesis: a global tectonic approach*. Unwin Hyman, Winchester, Massachusetts, USA. 57.



This work is licensed under a Creative Commons Attribution 4.0 International License CC BY. To view a copy of this license, visit <http://creativecommons.org/licenses/by/4.0/>

